Contribution from the Department of Chemistry,
State University of New York at Albany, Albany, New York 12222

# Steric Control of Aggregation in Neutral Silver(I) Thiolates, $[AgSR]_n$. Crystal and Molecular Structures of $[AgSCH(SiMe_3)_2]_8$, a Discrete Molecular Biscycle of Weakly Interacting $[AgSCH(SiMe_3)_2]_4$ Units, and of $[AgSC(SiPhMe_2)_3]_3$ and $[AgSC(SiMe_3)_3]_4$, Discrete Molecular Monocycles Containing Linearly Coordinated Silver(I) and Doubly Bridging Mercapto Sulfur Donors from Novel Sterically Hindered Thiolate Ligands. A Comparison with the Nonmolecular Structure of $[Ag_4\{SCH_2(SiMe_3)\}_3]_n(OMe)_n$[1]

Kaluo Tang,[†] Mohammad Aslam, Eric Block,* Terrence Nicholson, and Jon Zubieta*

*Received October 10, 1986*

By the use of a novel series of sterically hindered thiolate ligands, $(RR'R''Si)_nCH_{3-n}SH$, the colorless silver-thiolate complexes $[AgSC(SiMe_2Ph)_3]_3$ (**5a**) and $[AgSC(SiMe_3)_3]_4$ (**4a**) and the yellow species $[AgSCH(SiMe_3)_2]_8$ (**3a**) and $[Ag_4\{SCH_2(SiMe_3)\}_3(OCH_3)]_n$ (**2a**) have been synthesized and structurally characterized. The structure of **5a** consists of a discrete nonplanar six-membered cycle of alternating silver and sulfur atoms, $Ag_3S_3$, exhibiting no secondary Ag···S interactions between trinuclear units. In contrast, the structure of **4a** consists of a planar eight-membered cycle, $Ag_4S_4$, and exhibits unstrained digonal Ag-S coordination, unperturbed by secondary Ag···S interactions. The results suggest that a degree of control of aggregation may be introduced by employing ligands possessing sufficient steric bulk. Furthermore, the reduction of ligand steric hindrance in $^-SCH(SiMe_3)_2$ has profound structural consequences as illustrated by the structure of **3a**, which consists of two weakly interacting $[AgSCH(SiMe_3)_2]_4$ cycles, facing each other and connected by secondary Ag···S interactions, producing a T-shaped geometry about the Ag centers. Further reduction in the steric bulk of the ligand results in the polymeric structure of **2a**. The complex three-dimensional polymer may be described in terms of kinked chains of fused octanuclear $Ag_4S_4$ cyclic links cross-linked through bridging $Ag_4S_4$ monocycles. Crystal data: for **5a**, triclinic $P\bar{1}$, $a$ = 11.236 (2) Å, $b$ = 16.445 (3) Å, $c$ = 25.686 (4) Å, $\alpha$ = 92.79 (1)°, $\beta$ = 97.52 (1)°, $\gamma$ = 108.77 (1)°, $V$ = 4434.2 (9) Å$^3$, $D_{calcd}$ = 1.34 g cm$^{-3}$ for $Z$ = 2, $R$ = 0.061 for 9537 reflections; for **4a**, orthorhombic $Pbca$, $a$ = 17.478 (3) Å, $b$ = 28.314 (4) Å, $c$ = 29.706 (4) Å, $V$ = 14700.6 (12) Å$^3$, $D_{calcd}$ = 1.28 g cm$^{-3}$ for $Z$ = 8, $R$ = 0.069 for 2759 reflections; for **3a**, monoclinic $C2/c$, $a$ = 18.339 (4) Å, $b$ = 24.623 (4) Å, $c$ = 24.473 (4) Å, $\beta$ = 96.74 (1)°, $V$ = 10974.6 (11) Å$^3$, $D_{calcd}$ = 1.45 g cm$^{-3}$ for $Z$ = 4, $R$ = 0.063 for 3919 reflections; for **2b**, monoclinic $C2/c$, $a$ = 17.023 (3) Å, $b$ = 29.470 (5) Å, $c$ = 23.372 (4) Å, $\beta$ = 104.21 (1)°, $V$ = 11366.2 (14) Å$^3$, $D_{calcd}$ = 1.92 g cm$^{-3}$ for $Z$ = 16, $R$ = 0.069 for 1366 reflections.

We have recently developed several syntheses of (triorganosilyl)methanethiols, $(RR'R''Si)_nCH_{3-n}SH$ (**1**), making readily available members of this little studied class of compounds. Complementing the known[2] nucleophilic substitution approach to (trimethylsilyl)methanethiol (**2**) (Scheme I, step a, R = Me), we have utilized multiple silylation of the methanethiol carbanion equivalent (2-tetrahydropyranyl)(thiomethyl)lithium[3] in syntheses of bis- and tris(trimethylsilyl)methanethiol (**3** and **4**), respectively (Scheme I, step b), as well as conversion of **4** to **3** upon heating (Scheme I, step c)[4] and formation of **3** and **4** by reaction of bis- and tris(trimethylsilyl)methyllithium, respectively, with elemental sulfur (Scheme I, step d).[4]

Through use of the appropriate triorganosilyl chloride we have prepared such thiols as tris(dimethylphenylsilyl)methanethiol **5** (Scheme I, step d using $PhMe_2SiCl$) and bis(*tert*-butyldimethylsilyl)methanethiol[3] (**6**) (Scheme I, step b repeated twice using *t*-$BuMe_2SiCl$). The polysilylated thiols are of particular interest as representatives of a new class of hindered ligands with "tunable" steric demand. Variation in both the "R" groups as well as the number of silyl groups in structure **1** should lead to a corresponding variation in the steric cone angle[5] of the thiol. The polysilylated thiols are also of interest due to the $\beta$-effect of silicon,[6] an electron-releasing effect that should increase the electron density at sulfur compared to that in simple alkanethiols.[7] "Tuning" should also be possible here by changing the nature of the "R" groups and the number of silyl groups. Thiols **3** and **4** have recently been used in preparation of lithium[9a] and lead[9b] thiolates characterized by X-ray crystallography. We report here an X-ray crystallographic study of the silver thiolates of **2**-**5** in which a remarkable variation in aggregation states is seen.

Although a number of homoleptic $[Ag_x(SR)_y]^{x-y}$ silver thiolate complexes have been structurally characterized in recent years,[10-13] the types and structural patterns have not been fully realized. The anionic complexes $[Ag_5(SPh)_7]^{2-}$ and $[Ag_5(S\text{-}t\text{-}Bu)_6]^-$ occur as molecular cages with both two- and three-coordinate silver.[8,11,12] The hexaargentate species $[Ag_6(SPh)_8]_n^{2-}$ consists of a tubular

**Scheme I**

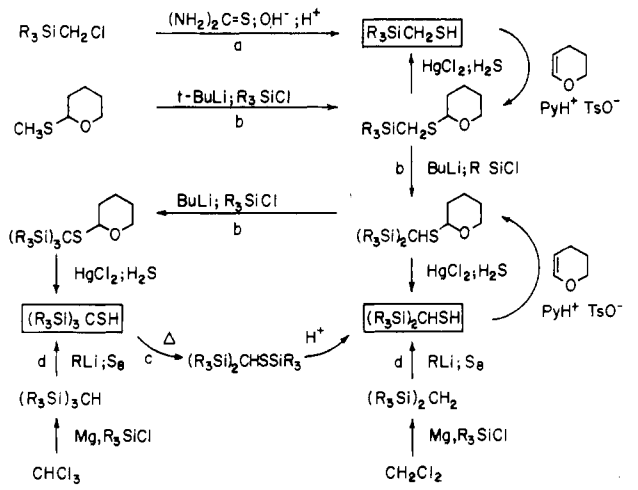


(1) Portions of this work have appeared in abstract form: Block, E. *XX Organosilicon Symposium*; Union Carbide Corp.: Tarrytown, NY, 1986. Block, E.; Zubieta, J. *Abstracts of Papers, 192nd* National Meeting of the American Chemical Society, Anaheim, CA; American Chemical Society: Washington, DC, 1986.
(2) Copper, G. D. *J. Am. Chem. Soc.* **1954**, *76*, 2500.
(3) Block, E. and Aslam, M. *J. Am. Chem. Soc.* **1985**, *107*, 6729.
(4) (a) Block, E.; Aslam, M. *Tetrahedron Lett.* **1985**, *26*, 2259. (b) Ricci, A.; Degl'innocenti, A.; Fiorenza, M.; Dembeck, P.; Ramadan, N.; Seconi, G.; Walton, D. R. M. *Tetrahedron Lett.* **1985**, *26*, 1091.
(5) Beattie, I. R.; Perle, J. *J. Chem. Soc. A* **1964**, 3627.
(6) (a) Colvin, E. W. *Silicon in Organic Synthesis*; Butterworths: London, 1981. (b) Jarvie, A. W. P. *Organomet. Chem. Rev., Sect. A* **1970**, *6*, 153.
(7) For example: (a) (Trimethylsilyl)methylamine shows enhanced basicity compared to (2,2-dimethylpropyl)amine.[6a] (b) The order of electron-donation toward the benzene ring has been found to be $(Me_3Si)_3C > (Me_3Si)_2CH > PhCH_2SiMe_2CH_2 > Bu_3SiCH_2 > Me_3SiCH_2 > Ph_3SiCH_2 > CH_3$.[8a,b] (c) (Trimethylsilyl)methanethiol shows enhanced reactivity in addition to alkynes compared to other alkanethiols.[6b]

* To whom correspondence should be addressed.
[†] Permanent address: Department of Chemistry, Beijing University, Beijing, The People's Republic of China.

0020-1669/87/1326-1488$01.50/0 

framework, composed of weakly associated $[Ag_{12}(SPh)_{16}]^{4-}$ units.[10] Uncharged compounds $[AgSR]_n$ are frequently insoluble, and to date only two $[AgSR]_n$ structural types have been described, the cyclic $[AgSC_6H_{11}]_{12}$, and the nonmolecular $[AgSCMeEt_2]_n$, which contains a chain of two intertwined but unconnected $[Ag(\mu\text{-}SR)]_n$ strands.[14] These observations suggest that the degree of aggregation of the silver thiolate species depends intimately upon both reaction conditions and the nature of the thiolate ligands. Akerstrom[15] has argued that the degree of association of $[AgSR]_n$ silver thiolate complexes is related to the chain branching at the thiolate $\alpha$-carbon atom. Thus, silver *tert*-alkanethiolates are octameric in solution while silver *sec*-alkanethiolates are dodecameric. Where there is less chain branching, insoluble, nonmolecular [AgSR] compounds are the rule. These observations suggest that thiolate ligands with sterically demanding substituents should exhibit a reduced tendency to bridge metal centers, thereby yielding discrete molecular species. Furthermore, the apparent correlation of degree of aggregation of $[AgSR]_n$ species with the steric bulk of the thiolate substituents R suggests that the size of molecular $[AgSR]_n$ cycles may be controlled by tuning the steric demands of the thiolate ligand.

In this paper we report the consequences of increasing steric bulk of the thiolate ligand on the structures of neutral homoleptic silver thiolates $[AgSR]_n$. The naive expectation that variation in the ligand volume will influence the degree of association $n$ appears justified, such that for $^-SC(SiMe_3)_3$ and $^-SC(SiMe_2Ph)_3$ we have characterized discrete tetrameric and trimeric species, $[AgSC(SiMe_3)_3]_4$ (**4a**) and $[AgSC(SiMe_2Ph)_3]_3$ (**5a**), respectively, while for the less hindered ligand $^-SCH(SiMe_3)_2$ we observe an octanuclear Ag unit $[AgSCH(SiMe_3)_2]_8$ (**3a**) composed of two weakly interacting $[AgSCH(SiMe_3)_3]_4$ monocycles.

Furthermore, the relatively unhindered thiolate $^-SCH_2(SiMe_3)$ yields a polymeric structure $[Ag_4\{SCH_2(SiMe_3)\}_3(OCH_3)]_n$, consisting of chains of linked $[Ag_4\{SCH_2(SiMe_3)\}_4]$ cycles, bridged by monocyclic $[Ag_4\{SCH_2(SiMe_3)\}_4]$ groups and weakly interacting methoxy groups.

## Experimental Section

Reagent grade chemicals were used throughout without further purification. Bis(trimethylsilyl)methanethiol and tris(trimethylsilyl)methanethiol were prepared by the published method.[4a]

Infrared spectra were recorded from KBr pellets with a Perkin-Elmer spectrometer and were referenced to the 1028-$cm^{-1}$ band of a 0.5-mm polystyrene film. $^1H$ NMR spectra were recorded on a Varian EM 360 or XL-300 spectrometer and were refernced internally to $(CH_3)_4Si$.

**Preparation of Tris(dimethylphenylsilyl)methanethiol, $(PhMe_2Si)_3$-CSH.** A solution of 4.18 g (0.01 mol) of $(Me_2PhSi)_3CH$[16] dissolved in 40 mL of dried THF in a flame-dried flask under argon was treated with 7.74 mL (0.012 mol) of $CH_3Li$ (1.55 M diethyl ether solution). After being stirred and heated to remove ether, the reaction mixture was refluxed for 6 h and subsequently cooled to room temperature. Sulfur (0.4 g, 0.012 mol) was added, and the mixture was refluxed for 1 h, cooled to room temperature, and stirred overnight. Addition of 20 mL of dilute $H_2SO_4$ saturated with sodium chloride resulted in the formation of a brown-red oil, which was extracted with 50 mL of benzene. The aqueous layer was extracted with three additional portions of benzene, and the combined benzene extracts were dried with $MgSO_4$, filtered, and concentrated. After addition of 50 mL of benzene, the solution was extracted with 50 mL of saturated KOH/methanol. Upon acidification of the basic extract with 10% HCl, a brown-orange oil separated. This oil was extracted with 50 mL of benzene, washed with $H_2O$, dried with $MgSO_4$, and evaporated to dryness. The residue was dissolved in 40 mL of hot hexane; this solution was filtered to remove insoluble impurities and cooled to room temperature. The pale yellow crystals that formed overnight were collected by filtration, washed with cold hexane, and dried. Recrystallization from hot hexane gave 0.39 g (10% yield) of pale yellow, nearly colorless crystals, mp 201–203 °C. $^1H$ NMR ($CDCl_3$): $\delta$ 0.21 (s, $CH_3$), 1.70 (s, SH), 7.1–7.55 (m, $-C_6H_5$); IR (KBr): 3040 (m), 3010 (m), 2950 (m), 2900 (m), 1955 (m), 1880 (m), 1820 (m), 1485 (m), 1425 (m), 1320 (m), 1300 (m), 1250 (s), 1100 (s), 930 (s), 885 (vs), 810 (vs), 790 (vs), 740 (s), 720 (s), 700 (vs), 630 (m), 470 (m), 390 (m), 345 (m) $cm^{-1}$.

**Preparation of $[AgSC(SiMe_2Ph)_3]_3$ (5a).** The reaction was carried out under argon in rigorously degassed solvents. To a well-stirred solution of $(Me_2PhSi)_3CSH$ (150 mg, 0.33 mmol) and $(C_2H_5)_3N$ (0.05 mL, 0.34 mmol) in benzene (10 mL) was added a solution of $AgNO_3$ (57 mg, 0.33 mmol) in acetonitrile (30 mL) at room temperature. The reaction mixture was refluxed for 2 h, sealed under argon, and stored overnight at 4 °C. The pale yellow microcrystals that formed were collected by filtration, washed with acetonitrile, and dried (yield 109 mg). A further crop (20 mg) of the same product was obtained from the mother liquor after further cooling. The total yield was 129 mg (65.5%). Preparations that were not refluxed after mixing of reactants gave poorer yields, ca. 30%, of microcrystalline product.

Recrystallization from benzene/acetonitrile afforded well-formed colorless crystals of cubic habit. IR (KBr): 3065 (m), 3045 (m), 2959 (m), 2902 (m), 1490 (m), 1425 (m), 1250 (ms), 1105 (ms), 836 (vs), 818 (sh), 790 (m), 735 (s), 700 (s), 470 (m), 430 (w), 390 (m), 370 (m) $cm^{-1}$.

**Preparation of $[AgSC(SiMe_3)_3]_4$ (4a).** To a stirred solution of $(Me_3Si)_3CSH$ (663 mg, 2.5 mmol) and $(C_2H_5)_3N$ (0.35 mL, 2.5 mmol) in acetonitrile (20 mL) was added a solution of $AgNO_3$ (425 mg, 2.5 mol) in acetonitrile (10 mL) at room temperature. The white precipitate, which formed immediately, was redissolved upon refluxing the mixture for 2 h. Cooling to room temperature yielded pale brown microcrystals, which were collected by filtration, washed with $CH_3CN$, and dried. Yield: 850 mg (91.5%).

The crude product (20 mg) was dissolved in 4 mL of hot ethanol and filtered to remove impurities. The colorless filtrate was evaporated slowly at room temperature for several days, whereupon colorless crystals of needle habit were obtained. The crystals are soluble in benzene, chloroform, THF, diethyl ether, and hot ethanol, slightly soluble in cold ethanol, and insoluble in acetonitrile; mp 235 °C dec. IR (KBr): 2960 (m), 2900 (m), 1410 (m), 1250 (s), 847 (vs), 824 (sh), 780 (m), 669 (s), 610 (m), 380 (m), 340 (m), 310 (m) $cm^{-1}$. NMR ($CDCl_3$): $\delta$ 0.51 (s, $CH_3$).

**Preparation of $[AgSCH(SiMe_3)_2]_8$ (3a).** All manipulations were carried out under argon. To a solution of $(Me_3Si)_2CHSH$ (0.481 g, 2.5 mmol) and $(C_2H_5)_3N$ (0.35 mL, 2.5 mmol) in acetonitrile (12 mL) was added a solution of $AgNO_3$ (0.425 g, 2.5 mmol) in acetonitrile (8 mL). From the resulting pale yellow reaction mixture, a yellow powder was observed to precipitate over a 4-h period. The powder was collected by filtration, washed with acetonitrile, and dried. The crude product was dissolved in hot ethanol and recrystallization effected by slow evaporation of solvent at room temperature to produce yellow crystals of cubic habit. Yield: 660 mg (88.0%). IR (KBr): 2960 (s), 2900 (m), 1440 (w), 1400 (w), 1250 (s), 1005 (s), 875–820 (broad, vs), 765 (s), 690 (m), 670 (w), 630 (w), 610 (w), 540 (w), 355 (m), 320 (w) $cm^{-1}$; NMR ($CDCl_3$): $\delta$ 0.33 (s, $CH_3$).

**Preparation of $[AgSCH_2(SiMe_3)]_n$ (2a) and $[Ag_4\{SCH_2(SiMe_3)\}_3]$-$(OMe)_n$ (2b).** Compound **2a** was prepared analogously to **3a**. The crude yellow product was recrysallized from hot chloroform to give thin filaments of composition $[AgSCH_2(SiMe_3)]$. Yield: 90%. Anal. Calcd: C, 21.2; H, 4.88; Found: C, 21.0; H, 4.94. IR (KBr): 2949 (s), 2889 (m), 1405 (m), 1380 (m), 1249 (m), 1012 (m), 860 (sh), 840 (vs), 780 (m), 755 (m), 690 (m), 640 (m), 450 (m), 320 (m) $cm^{-1}$; NMR ($CDCl_3$): $\delta$ 0.16 (s, $CH_3$), 2.11 (s, $CH_2$).

Attempts to grow X-ray quality crystals from a chloroform/methanol mixture yielded a material analyzing for $[Ag_4\{SCH_2(SiMe_3)\}_3(OMe)]$. Yield: 70%

**Collection and Reduction of X-ray Data and Solution and Refinement of the Structures.** The crystal data and experimental details of the structure determinations are given in Table I. A full description of the experimental details and of the methods of structure solution may be found in ref 17. None of the crystals exhibited significant decay under X irradiation, with a maximum of 5% for **2b**. Tables of bond lengths and angles, anisotropic temperature factors, calculated hydrogen atom pos-

(8) (a) Davis, D. D. *J. Organomet. Chem.* **1981**, *206*, 21. (b) The order of electron-donation by the $(Me_3Si)_3C$ and $(Me_3Si)_2CH$ groups may be reversed: Brough, L. F.; West, R. *J. Organomet. Chem.* **1982**, *229*, 113.
(9) (a) Aslam, M.; Barlett, R. A.; Block, E.; Olmstead, M. M.; Power, P. P.; Sigel, G. E. *J. Chem. Soc., Chem. Commun.* **1985**, 1674. (b) Hitchcock, P. B.; Jasim, H. A.; Kelly, R. E.; Lappert, M. *Ibid.* **1985**, 1776.
(10) (a) Hong, S.; Olin, A.; Hesse, R. *Acta Chem. Scand., Ser. A* **1975**, *A29*, 583. (b) Dance, I. G. *Inorg. Chim. Acta* **1977**, *25*, L17.
(11) Bowmaker, G. A.; Tan, L.-C. *Aust. J. Chem.* **1979**, *32*, 1443.
(12) Dance, I. G. *Aust. J. Chem.* **1978**, *31*, 2195.
(13) Dance, I. G. *Inorg. Chem.* **1981**, *20*, 1487.
(14) Dance, I. G.; Fitzpatrick, L. J.; Rae, A. D.; Scudder, M. L. *Inorg. Chem.* **1983**, *22*, 3785.
(15) Akerstrom, S. *Ark. Kemi* **1965**, *24*, 505.
(16) Eaborn, C.; Mansom, A. I. *J. Chem. Soc. Perkin Trans. 2* **1985**, 729.
(17) Bruce, A.; Corbin, J. L.; Dahlstrom, P. D.; Hyde, J. R.; Minelli, M.; Stiefel, E. I.; Spence, J. T.; Zubieta, J. *Inorg. Chem.* **1982**, *21*, 917.

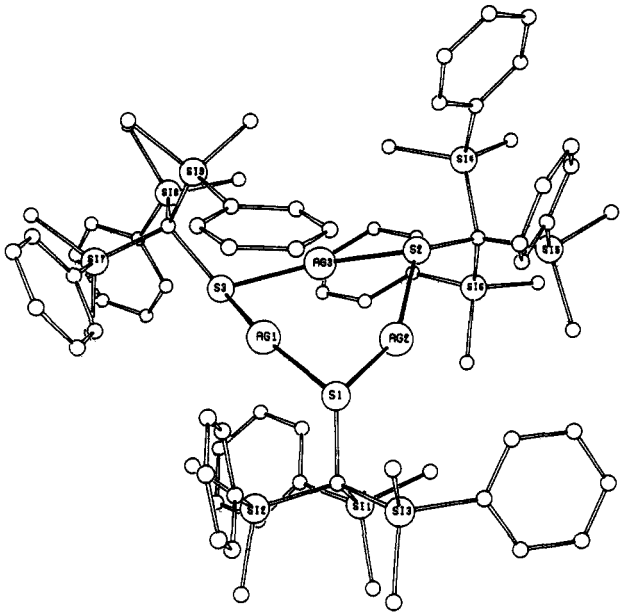

**Figure 1.** Perspective view of the structure of $[AgSC(SiMe_2Ph)_3]_3$ (**5a**).

itions, and calculated and observed structure factors are available as supplementary material.

## Results and Discussion

**Synthesis and Physical and Spectroscopic Properties.** Neutral homoleptic silver thiolate complexes are frequently insoluble, forming nonmolecular aggregates $[AgSR]_\infty$. On the other hand, compounds with branched-chain alkanethiol substituents have been shown to be readily soluble in common organic solvents.[10b,14] Both solution and solid-state observations demonstrate the significant stereochemical influence of the thiolate substituent in determining structures and degree of aggregation. The suggestion is that thiol substituents with significant steric cone angles[5] will stabilize cyclic $[AgSR]_n$ compounds of reduced ring sizes. The pronounced steric requirements of the ligands $(R_3Si)_3CSH$ are evident in the steric angles of ca. 120°, when compared to a value of ca. 85° for $(CH_3)_3CSH$. One member of this class, tris(trimethylsilyl)-methanethiol has already proven of interest in affording novel lithium[9a] and lead thiolates.[9b]

Ligand synthesis has been accomplished by deprotonation at the methyl position of a tris(triorganosilyl)methane by an alkyllithium, followed by addition of sulfur and acidification or by multiple metalation and silylation of the methanethiol carbanion equivalent 2-(methylthio)tetrahydropyran, as illustrated in Scheme I.

Reaction of the thiolate ligand with an equivalent amount of silver nitrate in ethanol, containing triethylamine as base, affords crystals of the silver thiolate derivatives, $[AgSR]_n$. In the case of **2** the mixed methoxy thiolate $[Ag_4\{SCH_2(SiMe_3)\}_3]_n(OMe)_n$ was isolated from a chloroform/methanol mixture. Compounds **3a**, **4a**, and **5a**, are soluble in common organic solvents, while **2a** and **2b** are soluble only in hot chloroform or methylene chloride. The crystalline solids are homogeneous in composition, and powder diffraction studies confirm the presence of a single crystalline modification for each of the derivatives.

The infrared spectra of the complexes exhibit strong bands in the 700–900-$cm^{-1}$ range, characteristic of the $R_3Si$ group. In addition, weak- and medium-intensity absortions in the 320–390-$cm^{-1}$ region may be assigned to $\nu$(AgS).

The crystalline compounds **4a** and **5a** are colorless while **2a**, **2b**, and **3a** are yellow. Although $[AgSR]_n$ species are either colorless or yellow, only those silver thiolates possessing trigonal silver or displaying secondary Ag···S interactions are yellow.[11] In those cases where only digonal silver coordination is present, the species are colorless, suggesting that absorption due to charge transfer from thiolate to linearly coordinated silver occurs at higher energy than that to trigonally coordinated silver.[14] The digonal coordination observed in the structures of **4a** and **5a** contrasts with

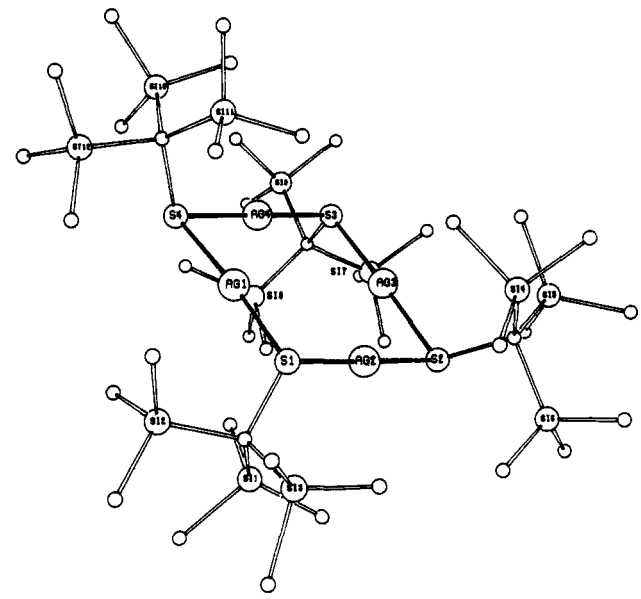

**Figure 2.** ORTEP diagram of the structure of $[AgSC(SiMe_3)]_4$ (**4a**). Methyl groups have been omitted for clarity.

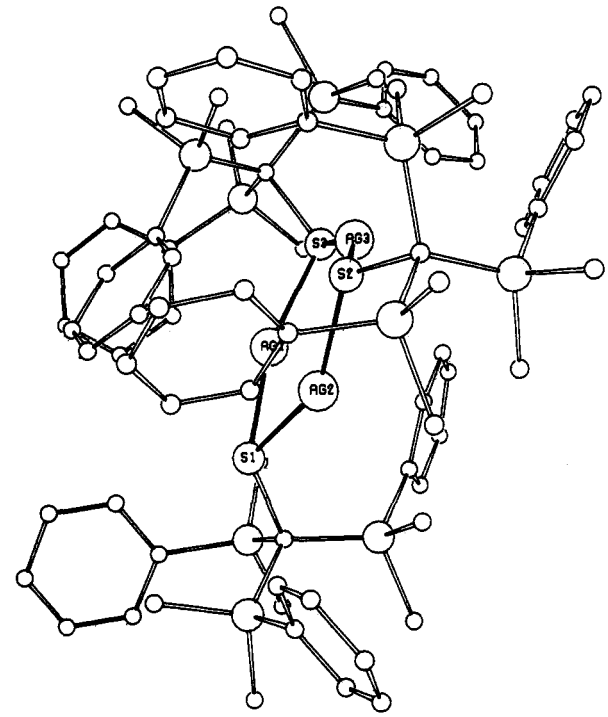

**Figure 3.** View of the $[AgSC(SiMe_2Ph)_3]_3$ monocycle showing the disposition of silyl substituents about the $Ag_3S_3$ core.

the T-shaped Ag centers of **3a** and the trigonal Ag units of **2b**, confirming these trends.

**Solid-State Structures.** The structures of $[AgSC(SiMe_2Ph)_3]_3$ (**5a**), $[AgSC(SiMe_3)_3]_4$ (**4a**), $[AgSCH(SiMe_3)_2]_8$ (**3a**), and $[Ag_4\{SCH_2(SiMe_3)\}_3(OMe)]$ (**2b**) are illustrated in Figures 1, 2, 4, and 6, respectively. Atomic positional and isotropic thermal parameters are presented in Tables II–V for **5a**, **4a**, **3a**, and **2a** respectively. Selected bond lengths and angles for the Ag clusters are compared in Table VI.

As illustrated in Figure 1, the structure of **5a** consists of a discrete six-membered cycle of alternating silver and sulfur atoms, $Ag_3S_3$. The silver–thiolate sulfur monocycle is distinctly puckered, with S2 ca. 0.50 Å from the least-squares plane through the silver atoms and S1 and S3. The silver atoms exhibit a coordination number of two with distorted digonal geometry. The S1–Ag1–S3 angle approaches the linear limit, while the valence angles at Ag2 and Ag3 are somewhat more contracted, 149.9 (1)° and 153.6

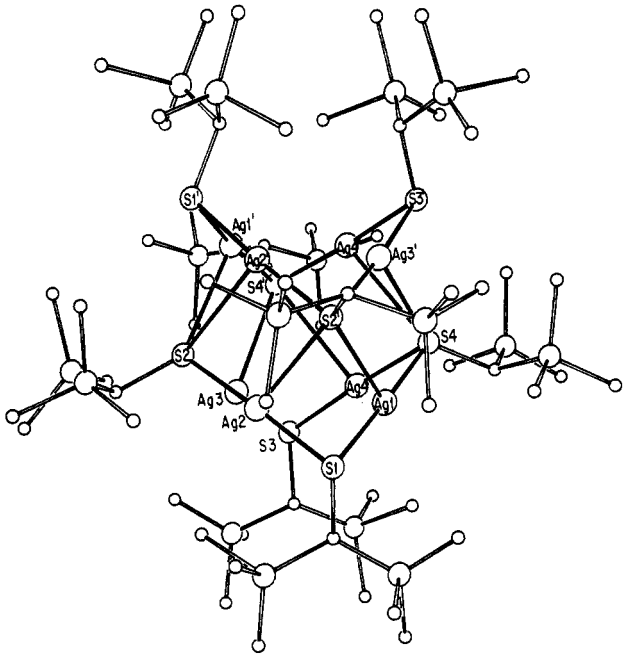


**Figure 4.** Perspective view of the structure of $\{[AgSCH(SiMe_3)_2]_4\}_2$ (**3a**) showing secondary Ag···S interactions.

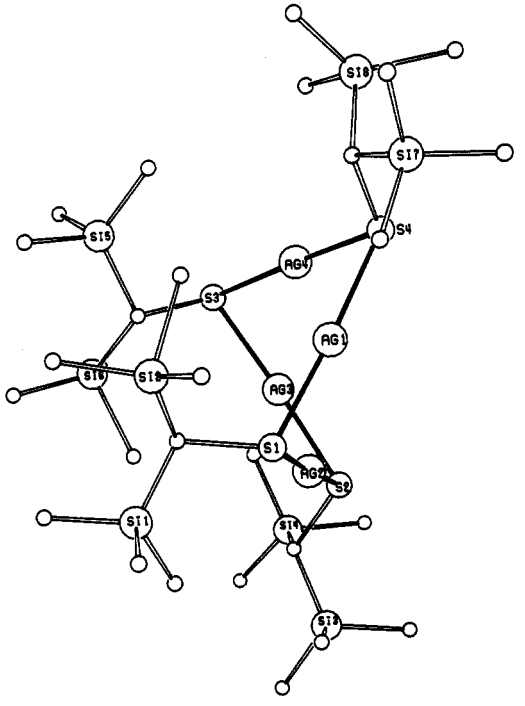


**Figure 5.** View of the isolated monocycle $[AgSCH(SiMe_3)_2]_4$.

(1)°, respectively. The preferred coordination number for silver(I) with thiolate ligands is two with linear geometry strongly favored. The irregular geometry displaced by the $Ag_3S_3$ framework is the consequence of constraints imposed by ring closure. Table VIII compares the bonding parameters for the $[Ag_3S_3]$ ring with those reported for the unconstrained one-dimensional nonmolecular structure of $[AgSR]_\infty$ (SR = 3-methylpentane-3-thiol[14]) and with the more relaxed cyclic structures $[AgSC_6H_{11}]_{12}$, $[AgSC(SiMe_3)_3]_4$ (**4a**), and $[AgSCH(SiMe_3)_2]_8$ (**3a**). The $Ag_3S_3$ ring geometry of **5a** is irregular, with Ag1 most closely approaching linear coordination but displaying significantly longer Ag–S bond distances than those associated with other examples of digonal Ag–S coordination. The Ag1···Ag distances are similar to those observed for the dodecameric cyclohexyl derivative $[AgSC_6H_{11}]_{12}$, while the Ag2···Ag3 distance is significantly longer (0.21 Å) and comparable to those of the nonmolecular structure $[AgSC_6H_{13}]_\infty$.

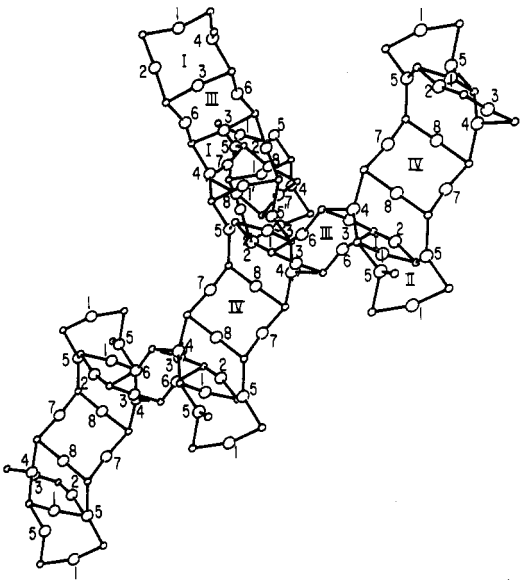

**Figure 6.** View of the polymeric structure of $[Ag_4\{SCH_2(SiMe_3)\}_3]_n(OCH_3)_n$ (**2b**) showing a strand of fused $Ag_4S_4$ cycles (I–III) cross-linked to adjacent strands through bridging $Ag_4S_4$ monocycles (IV).

Considerable variation has been observed in nonbonding Ag–Ag distances of silver–thiolate species, but no meaningful correlation is apparent between Ag–Ag distances and either the coordination number of the silver or the degree of aggregation of the cycle. Although a triangular arrangement of silver atoms has also been observed in the structure of $[Rh_3Ag_3H_9(tripod)_3]^{3+}$,[18] the Ag–Ag distances for this species are nearly identical and significantly shorter, exhibiting an average distance of 2.985 (6) Å with a range of 2.968 (4)–2.998 (4) Å.

The puckering of the $Ag_3S_3$ ring is a consequence of the angular requirements of the digonally coordinated silver and of the doubly bridging sulfur donors. A planar arrangement with linear S–Ag–S segments would require an unreasonably acute Ag–S–Ag angle of ca. 60°, while the limiting planar unit with a relaxed Ag–S–Ag angle of 90° would require an unusually contracted S–Ag–S angle of 150°. The observed irregular and puckered ring geometry is a compromise between extreme angles at S and Ag.

As illustrated in Figure 3, the $(Me_2PhSi)_3CS$ ligands project significant steric cones about the $Ag_3S_3$ ring, and preclude the formation of any secondary intercycle Ag···S interactions. In addition, the steric bulk of the ligand is such that a cyclic structure with $n > 3$ is unlikely, both as a consequence of increased intracycle steric interactions and also as a result of the severe steric constraints that may prevent the approach of independent fragments with $n \geq 2$ during the complexation and aggregation process.

It would appear that a molecular cycle with $n = 3$ represents a lower limit for species of the type $[AgSR]_n$. A four-membered $[Ag_2S_2]$ ring, $n = 2$, would preclude digonal coordination at silver, resulting in secondary Ag···S interactions between rings and hence a more complex aggregate structure.

The structure of **4a** consists of a discrete eight-membered cycle of alternating silver and sulfur atoms, $Ag_4S_4$, arranged in a shallow crown with a maximum deviation of 0.1 Å from the least-squares plane through the eight atoms. The ring geometry is much more regular than that observed for **5a** as a consequence of the angular relaxation allowed by the increased ring size. The S–Ag–S angles approach the digonal limit, and the angles at the bridging S atoms fall within the range observed for Ag–S–Ag interactions (Table VI). As with the structure of **5a**, the rings are discrete molecular units, exhibiting no secondary Ag···S interactions. The steric demands of the thiolate ligand prevent close approach of the tetranuclear silver units and preclude concomitant Ag···S bridging interactions to form oligomeric aggregates. In this sense, the

(18) Bachechi, F.; Ott, J.; Venanzi, L. M. *J. Am. Chem. Soc.* **1985**, *107*, 1760.

**Table I.** Summary of Crystal Data and Experimental Details for the Structural Studies of $[AgSC(SiMe_2Ph)_3]_3$, $[AgSC(SiMe_3)_3]_4$, $[AgSCH(SiMe_3)_2]_8$, and $[Ag_4[SCH_2(SiMe_3)]_3(OMe)]$

| | $[AgSC(SiMe_2Ph)_3]_3 \cdot 0.5C_6H_6$ (**5a**) | $[AgSC(SiMe_3)_3]_4$ (**4a**) | $[AgSCH(SiMe_3)_2]_8$ (**3a**) | $[Ag_4[SCH_2(SiMe_3)]_3]_n(OMe)_n$ (**2b**) |
|---|---|---|---|---|
| | (A) Crystal Parameters[a] at 23 °C | | | |
| $a$, Å | 11.236 (2) | 17.478 (3) | 18.339 (4) | 17.023 (3) |
| $b$, Å | 16.445 (3) | 28.314 (4) | 24.623 (4) | 29.470 (5) |
| $c$, Å | 25.686 (4) | 29.706 (4) | 24.473 (4) | 23.372 (4) |
| $\alpha$, deg | 92.79 (1) | 90.00 | 90.00 | 90.00 |
| $\beta$, deg | 97.52 (1) | 90.00 | 96.74 (1) | 104.21 (1) |
| $\gamma$, deg | 108.77 (1) | 90.00 | 90.00 | 90.00 |
| $v$, Å$^3$ | 4434.2 (9) | 14700.6 (12) | 10974.6 (11) | 11366.2 (14) |
| space group | $P\bar{1}$ | $Pbca$ | $C2/c$ | $C2/c$ |
| $Z$ | 2 | 8 | 4 | 16 |
| $D_{calcd}$,[g] g/cm$^3$ | 1.34 | 1.28 | 1.45 | 1.92 |
| $F(000)$ | 1767.0 | 6144.0 | 4864.0 | 6401.0 |
| | (B) Measurement of Intensity Data | | | |
| cryst dimens, mm | 0.20 × 0.21 × 0.22 | 0.12 × 0.08 × 0.07 | 0.19 × 0.21 × 0.18 | 0.25 × 0.06 × 0.25 |
| instrument | Nicolet R3m | Nicolet R3m | Nicolet R3m | Nicolet R3m |
| radiation | Mo K$\alpha$ ($\lambda$ = 0.71069 Å) | Mo K$\alpha$ ($\lambda$ = 0.71069 Å) | Mo K$\alpha$ ($\lambda$ = 0.71069 Å) | Mo K$\alpha$ ($\lambda$ = 0.71069 Å) |
| scan mode | coupled $\theta$(cryst)–$2\theta$(counter) | coupled $\theta$(cryst)–$2\theta$(counter) | coupled $\theta$(cryst)–$2\theta$(counter) | coupled $\theta$(cryst)–$2\theta$(counter) |
| scan rate, deg/min | 7–30 | 7–30 | 7–30 | 7–30 |
| scan range, deg | $0 < 2\theta \leq 45$k | $0 < 2\theta \leq 45$ | $0 < 2\theta \leq 45$ | $0 < 2\theta \leq 45$ |
| scan length | *h* | *h* | *h* | *h* |
| bkgd meas | *i* | *i* | *i* | *i* |
| stds | 3 collcd every 197 | 3 collcd every 197 | 3 collcd every 197 | 3 collcd every 197 |
| no. of reflcns collcd | 16063 | 9432 | 9309 | 3454 |
| no. of independent reflcns used in solution | 9537; $I_o \geq 3\sigma(I_o)$ | 2759; $I_o \geq 3\sigma(I_o)$ | 3919; $I_o \geq 3\sigma(I_o)$ | 1366; $I_o \geq 3\sigma(I_o)$ |
| | (C) Reduction of Intensity Data and Summary of Structure Solution and Refinement[b] | | | |
| abs coeff, cm$^{-1}$ | 8.77 | 13.71 | 17.32 | 15.67 |
| abs cor | *j* | *j* | *j* | *j* |
| struct solution: | *k* | *k* | *k* | *k* |
| atom scattering factors[c] | *c* | *c* | *c* | *c* |
| anomalous dispersion[d] | final discrepancy factor[e] | | | |
| $R$ | 0.061 | 0.069 | 0.063 | 0.069 |
| $R_w$ | 0.068 | 0.069 | 0.072 | 0.069 |
| goodness of fit[f] | 1.84 | 1.45 | 1.45 | 1.520 |

[a] From a least-squares fitting of the setting angle of 25 reflections. [b] All calculations were performed on a Data General Nova 3 computer with 32K of 16-bit words using local versions of the Nicolet SHELXTL interactive crystallographic software package as described in: Sheldrick, G. M. *Nicolet SHELXTL Operations Manual*; Nicolet XRD Corp.; Cupertino, CA 1979. Data were corrected for background, attenuators, and Lorentz and polarization effects in the usual fashion. [c] Neutral atomic scattering factors were used throughout the analysis: Cromer, D. T.; Mann, J. B. *Acta Crystallog., Sect. A: Cryst. Phys., Diffr., Theor. Gen. Crystallogr.* **1968**, *24*, 321. [d] Applied to all non-hydrogen atoms: *International Tables for X-ray Crystallography*; Kynoch: Birmingham, England, 1962; Vol. III. [e] $R = \sum[|F_o| - |F_c|/\sum|F_o|)$; $R_w = [\sum w(|F_o| - |F_c|)^2/\sum w|F_o|^2]^{1/2}$ where $w = 1/\delta^2(F_o) + g^*(F_o)$: $g = 0.0002$ for **5a**, $g = 0.001$ for **4a**, $g = 0.0005$ for **3a**, and $g = 0.0001$ for **2a**. [f] GOF $= [\sum w(|F_o| - |F_c|)^2/(NO - NV)]^{1/2}$ where NO is the number of observations and NV is the number of variables. [g] Densities were not measured. [h] From $[2\theta(K\alpha_1) - 1.0]$ to $[2\theta(K\alpha_2) + 1.0]°$. [i] Stationary crystal, stationary counter, at the beginning and end of each $2\theta$ scan, each for the time taken fro the scan. [j] Based on $\psi$ scans for five reflections with $\chi$ angles near 90 or 270°. [k] Patterson synthesis yielded the Ag position; all remaining non-hydrogen atoms were located via standard Fourier technique.

structure may be compared to that of $(Ph_3P)_4(AgSBu\text{-}t)_{14}$ [19]where a 28-membered cycle of alternating silver and sulfur atoms is formed, again with no evidence of secondary Ag···S interactions. In this latter case, strand entwinement prevents aggregation through secondary Ag···S interaction.

A cyclic structural unit $[Ag_4(\mu\text{-}SR)_4]$ has been identified in association with a $(Ph_3PAg)_2Ag_2(\mu\text{-}SR)_4$ unit in the structure of $(Ph_3P)_2(AgSCMeEt_2)_8$.[19] In contrast to **4a**, this eight-membered cycle is distinctly nonplanar and is connected by weak Ag–S bonds to the phosphine-containing segment. The isolation of a discrete monocycle for $[AgSC(SiMe_3)_3]_4$ confirms that ligand steric demands may minimize secondary Ag···S interactions, although the size of the cycle may depend on both reaction conditions[22] and the nature of the steric demands imposed by the ligand.

It is apparent from the structures of **5a** and **4a** and from previously reported examples of $[AgSR]_n$ structural types that the steric demands of the thiolate substituent R have a profound influence on the degree of association of the silver(I) organothiolate. To a first approximation, the entropic factor should promote cyclization in $[AgSR]_n$ aggregates.[23] On the other hand, secondary Ag···S interactions will oppose the formation of discrete molecular cycles, providing a driving force for further aggregation and polymerization. Thus, silver(I) alkanethiolates with unbranched chains are high polymeric compounds, since the silver centers are unprotected from the approach of additional, potentially bridging, thiolate groups. Simple branched-chain alkanethiol ligands afford a degree of steric protection to the silver centers, as demonstrated by the formation of discrete octameric and dodecameric cycles in solution. However, the steric cones associated with these ligands are insufficient to shield the ring units effectively. Hence, the molecular $[AgSR]_8$ unit of (3-methylpentane-3-thiolato)silver in solution is lost upon crystallization to give a nonmolecular $[AgSR]_\infty$ structure, although the remnants of the cyclic octameric molecules are present as crossover sections in the crystal structure. It would appear that the simple branched alkyl group of the thiolate ligand does not afford the steric pro-

(19) Dance, I.; Fitzpatrick, L.; Scudder, M.; Craig, D. *J. Chem. Soc., Chem. Commun.* **1984**, 17.
(20) Kunchar, N. R. *Nature (London)* **1964**, *204*, 468.
(21) Bradley, D. C.; Kunchar, N. R., unpublished results cited in ref 6.
(22) Watson, A. D.; Rao, Ch. P.; Dorfman, J. R.; Holm, R. H. *Inorg. Chem.* **1985**, *24*, 2820.
(23) Seeman, N. C. *J. Biomol. Struct. Dyn.* **1985**, *3*, 11.

**Table II.** Atom Coordinates ($\times 10^4$) and Temperature Factors ($Å^2 \times 10^3$) for $[AgSC(SiMe_2Ph)]_3$ (**5a**)

| atom | x | y | z | $U_{equiv}$ | atom | x | y | z | $U_{equiv}$ |
|---|---|---|---|---|---|---|---|---|---|
| Ag1 | 6147 (1) | 3153 (1) | 2178 (1) | 44 (1)[a] | C47 | 2860 (10) | −820 (6) | 1285 (4) | 52 (2) |
| Ag2 | 5217 (1) | 1912 (1) | 2978 (1) | 46 (1)[a] | C48 | 1480 (10) | −2266 (7) | 1918 (4) | 64 (3) |
| Ag3 | 4135 (1) | 1450 (1) | 1730 (1) | 43 (1)[a] | C51 | 5303 (9) | −529 (6) | 3413 (4) | 53 (2) |
| S1 | 6818 (2) | 3326 (1) | 3167 (1) | 35 (1)[a] | C52 | 6148 (10) | 628 (7) | 3612 (4) | 69 (3) |
| S2 | 4306 (2) | 545 (1) | 2437 (1) | 39 (1)[a] | C53 | 7479 (11) | 478 (7) | 3753 (5) | 83 (3) |
| S3 | 4877 (2) | 2732 (1) | 1277 (1) | 32 (1)[a] | C54 | 7914 (13) | −173 (8) | 3685 (5) | 102 (4) |
| Si1 | 4701 (2) | 3959 (1) | 3554 (1) | 43 (1)[a] | C55 | 7157 (12) | −1021 (8) | 3513 (5) | 98 (4) |
| Si2 | 7344 (2) | 5260 (1) | 3317 (1) | 40 (1)[a] | C56 | 5777 (11) | −1215 (7) | 3371 (5) | 83 (3) |
| Si3 | 7304 (2) | 4121 (1) | 4317 (1) | 42 (1)[a] | C57 | 3215 (10) | −69 (7) | 3851 (4) | 72 (3) |
| Si4 | 2927 (2) | −1252 (1) | 1980 (1) | 42 (1)[a] | C58 | 2704 (11) | −1887 (7) | 3351 (5) | 79 (3) |
| Si5 | 3540 (3) | −715 (2) | 3274 (1) | 50 (1)[a] | C61 | 756 (10) | 38 (6) | 1838 (4) | 48 (2) |
| Si6 | 1425 (3) | −162 (2) | 2544 (1) | 47 (1)[a] | C62 | 1033 (9) | 865 (6) | 1863 (4) | 59 (2) |
| Si7 | 6379 (2) | 3763 (1) | 471 (1) | 36 (1)[a] | C63 | 517 (11) | 1022 (7) | 1161 (4) | 75 (3) |
| Si8 | 4300 (2) | 1941 (1) | 118 (1) | 36 (1)[a] | C64 | −288 (11) | 331 (7) | 776 (5) | 77 (3) |
| Si9 | 6883 (2) | 2020 (1) | 848 (1) | 36 (1)[a] | C65 | −566 (11) | −489 (7) | 942 (5) | 79 (3) |
| C1 | 6487 (8) | 4185 (5) | 3596 (3) | 33 (2) | C66 | −62 (9) | −643 (6) | 1471 (4) | 62 (3) |
| C2 | 2956 (8) | −423 (6) | 2563 (4) | 36 (2) | C67 | 148 (10) | −1072 (7) | 2782 (4) | 73 (3) |
| C3 | 5676 (6) | 2601 (4) | 679 (3) | 31 (1) | C68 | 1589 (10) | 832 (7) | 2980 (4) | 73 (3) |
| C11 | 3931 (10) | 4109 (7) | 2855 (4) | 46 (3) | C71 | 8049 (7) | 4365 (4) | 829 (3) | 36 (2) |
| C12 | 3446 (8) | 3391 (5) | 2443 (4) | 56 (2) | C72 | 8221 (7) | 4805 (5) | 1359 (3) | 44 (2) |
| C13 | 2899 (11) | 3488 (8) | 1912 (5) | 68 (3) | C73 | 9430 (9) | 5296 (6) | 1625 (4) | 56 (2) |
| C14 | 2892 (13) | 4315 (9) | 1801 (5) | 82 (4) | C74 | 10478 (9) | 5367 (6) | 1366 (4) | 55 (2) |
| C15 | 3276 (13) | 4989 (8) | 2188 (5) | 81 (4) | C75 | 10328 (9) | 4959 (6) | 858 (4) | 52 (2) |
| C16 | 3841 (12) | 4926 (8) | 2740 (5) | 68 (3) | C76 | 9125 (7) | 4466 (5) | 590 (3) | 45 (2) |
| C17 | 4339 (11) | 4715 (7) | 4061 (5) | 65 (3) | C77 | 5376 (8) | 4444 (6) | 629 (4) | 50 (2) |
| C18 | 3785 (9) | 2840 (6) | 3719 (4) | 56 (2) | C78 | 6485 (8) | 3781 (5) | −283 (4) | 52 (2) |
| C21 | 9120 (7) | 5525 (5) | 3464 (3) | 42 (3) | C81 | 3203 (7) | 2553 (5) | −121 (3) | 39 (2) |
| C22 | 9877 (10) | 6161 (6) | 3865 (4) | 49 (2) | C82 | 3049 (8) | 2769 (6) | −658 (4) | 53 (2) |
| C23 | 11199 (10) | 6316 (6) | 3993 (4) | 52 (2) | C83 | 2135 (10) | 3158 (6) | −844 (4) | 69 (3) |
| C24 | 11759 (11) | 5852 (7) | 3705 (5) | 64 (3) | C84 | 1411 (10) | 3340 (7) | −494 (4) | 74 (3) |
| C25 | 11032 (11) | 5216 (7) | 3276 (5) | 64 (3) | C85 | 1502 (10) | 3151 (6) | 30 (4) | 70 (3) |
| C26 | 9705 (10) | 5057 (7) | 3163 (4) | 49 (2) | C86 | 2411 (8) | 2738 (5) | 226 (4) | 53 (2) |
| C27 | 6998 (9) | 6214 (6) | 3632 (4) | 60 (2) | C87 | 4887 (8) | 1580 (5) | −492 (4) | 54 (2) |
| C28 | 6923 (8) | 5243 (5) | 2555 (4) | 53 (2) | C88 | 3214 (8) | 936 (5) | 347 (4) | 44 (2) |
| C31 | 6356 (7) | 3177 (5) | 4655 (3) | 44 (2) | C91 | 7803 (7) | 2295 (5) | 1571 (3) | 39 (2) |
| C32 | 5640 (8) | 3291 (6) | 5064 (4) | 59 (2) | C92 | 7444 (8) | 1752 (5) | 1973 (4) | 51 (2) |
| C33 | 5000 (11) | 2567 (8) | 5336 (5) | 69 (3) | C93 | 8206 (9) | 1889 (6) | 2494 (4) | 64 (2) |
| C34 | 5059 (11) | 1776 (7) | 5221 (5) | 69 (3) | C94 | 9312 (9) | 2581 (6) | 2621 (4) | 66 (3) |
| C35 | 5774 (11) | 1654 (8) | 4813 (5) | 68 (3) | C95 | 9696 (9) | 3136 (6) | 2231 (4) | 63 (2) |
| C36 | 6432 (10) | 2354 (7) | 4545 (4) | 55 (2) | C96 | 8964 (8) | 2994 (5) | 1702 (4) | 50 (2) |
| C37 | 8914 (10) | 3998 (6) | 4330 (4) | 53 (2) | C97 | 8057 (8) | 2215 (5) | 352 (4) | 54 (2) |
| C38 | 7569 (10) | 5116 (6) | 4789 (4) | 54 (2) | C98 | 6106 (8) | 809 (5) | 798 (4) | 51 (2) |
| C41 | 4369 (8) | −1594 (5) | 2044 (3) | 48 (2) | Cs1 | 9759 (12) | 2145 (8) | 4898 (6) | 157 (6) |
| C42 | 5560 (10) | −1010 (7) | 2003 (4) | 52 (2) | Cs2 | 9536 (12) | 1682 (8) | 5231 (6) | 156 (6) |
| C43 | 6656 (9) | −1271 (6) | 2020 (4) | 60 (2) | Cs3 | 10049 (12) | 1058 (8) | 5297 (6) | 237 (11) |
| C44 | 6558 (11) | −2087 (7) | 2080 (4) | 75 (3) | Cs4 | 11266 (12) | 1157 (8) | 5018 (6) | 221 (10) |
| C45 | 5388 (12) | −2706 (8) | 2132 (5) | 95 (4) | Cs5 | 11517 (12) | 1789 (8) | 4714 (6) | 157 (7) |
| C46 | 4313 (11) | −2437 (7) | 2118 (4) | 72 (3) | Cs6 | 10778 (12) | 2217 (8) | 4583 (6) | 178 (8) |

[a] Equivalent isotropic $U$ defined as one-third of the trace of the orthogonalized $U_{ij}$ tensor.

tection to prevent the formation of secondary interactions and consequent aggregation as the species passes from the solution to the more dense crystalline phase. In a similar fashion, the crystal structure of (cyclohexanethiolato)silver reveals, not isolated dodecameric units $[AgSR]_{12}$, but cyclic molecules lapped over each other along the chain and displaying significant secondary Ag···S bonding between cycles, such that the structure was first described as a one-dimensional nonmolecular framework.[10a] Once again, ligand steric factors are not dominant, and secondary interactions in the crystal produce further aggregation of units.

With sufficiently bulky substituents, silver centers of a discrete cyclic unit should be completely shielded from secondary interactions, with the consequence that the molecular cyclic structure will be preserved. Furthermore, the steric constraints imposed by the substituent may determine the degree of association $n$ by restricting the approach of fragments during ring formation. The bulky tris(triorganosilyl)methane substituents of the new ligands, $(R_3Si)_3CSH$, provide sufficient steric congestion to accomplish both the prevention of secondary interactions between rings and the limitation of ring size.

In contrast, the less hindered thiolate $^-SCH(SiMe_3)_2$ is ineffective in preventing the approach of discrete $[AgSR]_n$ monocyclic units. This allows the formation of secondary *ag*···S interactions to produce the biscyclic structure $[AgSCH(SiMe_3)_2]_8$, illustrated in Figure 4. Furthermore, the $\beta$-effect of silicon, which may be at a maximum in this ligand, could promote secondary Ag···S interactions by enhancing the electron density at sulfur. The species may be formulated as $[\{AgSCH(SiMe_3)_2\}_4]_2$ since there are clearly two tetranuclear Ag cycles, which face each other and are connected by weak secondary Ag···S interactions, (Table VII). As shown in Figure 5, the $[AgSCH(SiMe_3)_2]_4$ unit is distinctly nonplanar, as a consequence of folding along the S1–S3 axis to give a dihedral angle of 78.0° between the best planes through S1Ag1S4Ag4S3 and S3AgS2Ag2S1. Each cycle contains four linear S–Ag–S segments, while intercycle connectivity is provided through eight Ag···S secondary interactions involving S2, S2′, S4, and S4′ exclusively. The geometry about the silver atoms is distinctly T-shaped, rather than trigonal planar.

The consequences of further reduction of the ligand bulk are dramatically illustrated by the structure of nonmolecular species $[Ag_4\{SCH_2(SiMe_3)\}_3]_n(OCH_3)]_n$ (**2b**), shown in Figure 6. The complex polymeric structure may be described in terms of one-dimensional kinked chains of fused octanuclear $Ag_4S_4$ cycles, I, II, and III, cross-linked through octanuclear $Ag_4S_4$ monocycles IV. A portion of the chain is shown in Figure 7a, along with schematics of the three crystallographically independent $Ag_4S_4$ cycles which fuse along opposite S-Ag-S edges to constitute one chain. As illustrated in Figure 8a, b, the octanuclear cycle

**Table III.** Atom Coordinates ($\times 10^4$) and Temperature Factors ($Å^2 \times 10^3$) for $[AgSC(SiMe_3)_3]_4$ (**4a**)

| atom | x | y | z | $U_{equiv}$ | atom | x | y | z | $U_{equiv}$ |
|---|---|---|---|---|---|---|---|---|---|
| Ag1 | 6612 (1) | 1255 (1) | 671 (1) | 56 (1)[a] | C16 | 8486 (18) | −604 (11) | −163 (10) | 98 (11) |
| Ag2 | 6575 (2) | 235 (1) | 1231 (1) | 71 (1)[a] | C17 | 6972 (19) | −714 (11) | 308 (11) | 103 (12) |
| Ag3 | 6232 (2) | 805 (1) | 2177 (1) | 75 (1)[a] | C18 | 6933 (23) | −245 (14) | −595 (13) | 156 (17) |
| Ag4 | 6341 (1) | 1825 (1) | 1628 (1) | 59 (1)[a] | C19 | 4636 (18) | 397 (10) | 1547 (10) | 89 (11) |
| S1 | 6715 (5) | 454 (3) | 456 (3) | 64 (4)[a] | C20 | 3822 (24) | −459 (16) | 1885 (15) | 37 (14) |
| S2 | 6413 (5) | −7 (3) | 1997 (3) | 79 (4)[a] | C21 | 5161 (22) | −603 (13) | 1067 (12) | 74 (13) |
| S3 | 6113 (5) | 1605 (3) | 2387 (2) | 70 (4)[a] | C22 | 4697 (22) | −839 (11) | 2896 (12) | 66 (12) |
| S4 | 6579 (4) | 2066 (2) | 872 (2) | 52 (3)[a] | C23 | 4523 (22) | 305 (12) | 2611 (14) | 86 (14) |
| Si1 | 8413 (8) | 263 (4) | 692 (4) | 82 (4) | C24 | 5958 (23) | −166 (15) | 3089 (13) | 85 (15) |
| Si2 | 7900 (7) | 770 (4) | −223 (4) | 76 (4) | C25 | 5574 (15) | −876 (9) | 1601 (8) | 60 (9) |
| Si3 | 7489 (7) | −313 (4) | −52 (4) | 85 (4) | C26 | 5661 (16) | −649 (9) | 2626 (10) | 72 (10) |
| Si4 | 4825 (11) | −292 (6) | 1661 (6) | 78 (6) | C27 | 6652 (25) | −1073 (15) | 1558 (13) | 113 (17) |
| Si5 | 5157 (11) | −246 (7) | 2712 (7) | 89 (7) | C28 | 7385 (18) | 1602 (10) | 3794 (9) | 91 (11) |
| Si6 | 6083 (12) | −996 (7) | 2079 (7) | 93 (7) | C29 | 7457 (17) | 813 (10) | 3122 (10) | 86 (11) |
| Si7 | 6901 (6) | 1358 (3) | 3271 (3) | 88 (3) | C30 | 5950 (18) | 1173 (12) | 3396 (11) | 119 (13) |
| Si8 | 7858 (6) | 1823 (3) | 2481 (3) | 89 (3) | C31 | 8032 (18) | 1304 (10) | 2115 (10) | 87 (11) |
| Si9 | 6608 (6) | 2413 (4) | 2985 (3) | 98 (4) | C32 | 8676 (19) | 1828 (13) | 2917 (11) | 129 (14) |
| Si10 | 5553 (5) | 2902 (3) | 1036 (3) | 57 (3) | C33 | 7949 (18) | 2364 (10) | 2120 (10) | 90 (11) |
| Si11 | 4902 (5) | 2015 (3) | 508 (3) | 70 (3) | C34 | 6274 (21) | 2800 (11) | 2516 (12) | 138 (14) |
| Si12 | 6199 (5) | 2655 (3) | 79 (3) | 70 (3) | C35 | 5760 (19) | 2355 (13) | 3341 (12) | 128 (14) |
| C1 | 7662 (13) | 300 (8) | 225 (7) | 35 (7) | C36 | 7382 (20) | 2714 (13) | 3272 (13) | 144 (16) |
| C2 | 5555 (12) | −381 (8) | 2082 (7) | 52 (7) | C37 | 5065 (16) | 3424 (9) | 780 (9) | 76 (10) |
| C3 | 6911 (13) | 1791 (9) | 2786 (7) | 41 (8) | C38 | 4904 (16) | 2699 (9) | 1491 (8) | 71 (10) |
| C4 | 5752 (6) | 2399 (7) | 617 (6) | 43 (7) | C39 | 6455 (15) | 3137 (9) | 1309 (9) | 74 (9) |
| C10 | 8355 (24) | −299 (12) | 986 (14) | 152 (17) | C40 | 4027 (16) | 2352 (10) | 431 (10) | 89 (11) |
| C11 | 8385 (18) | 797 (9) | 1067 (10) | 94 (11) | C41 | 4721 (18) | 1574 (10) | 952 (10) | 89 (11) |
| C12 | 9445 (20) | 355 (12) | 411 (11) | 129 (14) | C42 | 5021 (18) | 1642 (10) | −2 (9) | 90 (11) |
| C13 | 8311 (19) | 1335 (10) | 83 (11) | 107 (12) | C43 | 6908 (18) | 3110 (11) | 206 (11) | 105 (13) |
| C14 | 7047 (20) | 938 (11) | −548 (11) | 113 (13) | C44 | 6726 (16) | 2203 (9) | −270 (9) | 77 (10) |
| C15 | 8614 (19) | 531 (12) | −656 (11) | 122 (14) | C45 | 5427 (19) | 2946 (12) | −284 (11) | 121 (14) |

[a] Equivalent isotropic $U$ defined as one-third of the trace of the orthogonalized $U_{ij}$ tensor.

**Table IV.** Atom Coordinates ($\times 10^4$) and Temperature Factors ($Å^2 \times 10^3$) for $[AgSCH(SiMe_3)_2]_8$ (**3a**)

| atom | x | y | z | $U_{equiv}$ | atom | x | y | z | $U_{equiv}$ |
|---|---|---|---|---|---|---|---|---|---|
| Ag1 | 4359 (1) | 2205 (1) | 3426 (1) | 69 (1)[a] | C13 | 2309 (20) | 432 (14) | 4072 (13) | 268 (18) |
| Ag2 | 4056 (1) | 1297 (1) | 2555 (1) | 68 (1)[a] | C21 | 1512 (11) | 2016 (8) | 4053 (9) | 130 (8) |
| Ag3 | 3730 (1) | 2133 (1) | 1725 (1) | 70 (1)[a] | C22 | 3080 (14) | 1729 (11) | 4682 (11) | 190 (12) |
| Ag4 | 4013 (1) | 3035 (1) | 2585 (1) | 72 (1)[a] | C23 | 2846 (14) | 2666 (9) | 3911 (11) | 167 (10) |
| S1 | 3700 (2) | 1366 (2) | 3463 (1) | 64 (1)[a] | C31 | 4097 (12) | −82 (10) | 2058 (8) | 155 (9) |
| S2 | 4379 (2) | 1297 (1) | 1629 (2) | 61 (1)[a] | C32 | 3587 (15) | −395 (11) | 931 (11) | 195 (12) |
| S3 | 3030 (2) | 2931 (2) | 1862 (2) | 65 (1)[a] | C33 | 5124 (12) | 54 (10) | 1190 (10) | 163 (9) |
| S4 | 4948 (2) | 3077 (2) | 3360 (2) | 70 (1)[a] | C41 | 3346 (12) | 1776 (9) | 409 (9) | 145 (8) |
| Si1 | 2201 (4) | 846 (3) | 3261 (4) | 153 (4)[a] | C42 | 4664 (12) | 1130 (9) | 211 (10) | 149 (8) |
| Si2 | 2517 (4) | 1864 (4) | 4058 (3) | 151 (4)[a] | C43 | 3084 (14) | 667 (10) | 1 (10) | 173 (10) |
| Si3 | 4151 (3) | 112 (2) | 1325 (2) | 101 (2)[a] | C51 | 2442 (13) | 3835 (10) | 2775 (10) | 170 (10) |
| Si4 | 3726 (3) | 1069 (2) | 449 (2) | 107 (2)[a] | C52 | 1057 (10) | 3241 (8) | 2868 (8) | 114 (6) |
| Si5 | 1819 (3) | 3363 (3) | 2469 (3) | 126 (3)[a] | C53 | 1276 (20) | 3754 (15) | 1748 (14) | 274 (18) |
| Si6 | 1573 (3) | 2354 (3) | 1659 (2) | 135 (3)[a] | C61 | 683 (11) | 2164 (8) | 1854 (8) | 122 (7) |
| Si7 | 5204 (3) | 3339 (2) | 4572 (2) | 96 (2)[a] | C62 | 1591 (15) | 2530 (12) | 967 (11) | 191 (11) |
| Si8 | 4765 (5) | 4264 (3) | 3679 (4) | 132 (4)[a] | C63 | 2012 (14) | 1621 (10) | 1652 (11) | 179 (10) |
| C10 | 2692 (7) | 1485 (5) | 3424 (5) | 55 (3) | C71 | 6186 (9) | 3324 (8) | 4535 (7) | 112 (6) |
| C20 | 3810 (8) | 811 (6) | 1180 (6) | 71 (4) | C72 | 5033 (12) | 3780 (9) | 5167 (9) | 141 (8) |
| C30 | 2189 (7) | 2733 (5) | 2182 (5) | 58 (4) | C73 | 4895 (11) | 2661 (8) | 4768 (9) | 125 (7) |
| C40 | 4677 (9) | 3542 (6) | 3897 (6) | 77 (4) | C81 | 4226 (15) | 4393 (12) | 2981 (11) | 196 (12) |
| C11 | 1197 (10) | 941 (8) | 3093 (8) | 118 (7) | C82 | 5817 (18) | 4404 (13) | 3650 (14) | 258 (17) |
| C12 | 2553 (18) | 384 (13) | 2894 (13) | 244 (15) | C83 | 4147 (24) | 4616 (16) | 4096 (16) | 380 (27) |

[a] Equivalent isotropic $U$ defined as one-third of the trace of the orthogonalized $U_{ij}$ tensor.

Ag7S6Ag8S5Ag7′S6′Ag8′S5′ cross-links adjacent kinked strands into a complex three-dimensional structure.

The one-dimensional chain is severely kinked as a consequence of trigonal-planar coordination at Ag4 and Ag5 (Table IX), which form exocyclic bonds to S5 and S6, respectively. In turn these sulfur donors S5 and S6 are incorporated into the cross linking $Ag_4S_4$ monocycle IV (Figure 8b). Cycle II is most severely distorted from planar geometry, presenting as a distinct butterfly, bent along the Ag5–S2 axis (Figure 7c); this distortion results from the presence of two trigonal silver centers in the octanuclear unit. Although cycle I (Figure 7b) is also nonplanar, the effect is less dramatic, producing a boat conformation with a shallow "bow" at Ag2 and high "poop" at Ag4. Cycles III and IV (Figures 7d and 8b), which possess digonal silver centers exclusively, are nearly planar with maximum deviations of ca. 0.08 Å from the respective $Ag_4S_4$ planes.

With the exception of Ag4 and Ag5, all silver centers are linearly coordinated to two bridging sulfur donors. Whereas the digonal silver centers exhibit an average Ag–S distance of 2.41 (4) Å, the trigonally coordinated Ag atoms exhibit an average distance of 2.53 (4) Å, a result consistent with those observed for the respective metal sites in $[AgSC_6H_n]_{12}$. All sulfur donors are triply bridging, to satisfy the coordination requirements of two trigonal Ag centers and six digonal Ag centers of the asymmetric unit, $[Ag_8\{SCH_2(SiMe_3)\}_6]^{2+}$.

Although the overall structure is polymeric with a silver–thiolate composition of $[Ag_8\{SCH_2(SiMe_3)\}_6]_n^{n(2+)}$, the remnants of cyclic tetrameric units $[AgSR]_4$ are evidenced in both the fused chain

**Table V.** Atom Coordinates ($\times 10^4$) and Temperature Factors ($Å^2 \times 10^3$) for $[Ag_4\{SCH_2(SiMe)\}_3]_n(OCH_3)_n$ (**2b**)

| atom | x | y | z | $U_{equiv}$ | atom | x | y | z | $U_{equiv}$ |
|---|---|---|---|---|---|---|---|---|---|
| Ag1 | 5602 (3) | 1294 (2) | 3353 (2) | 56 (2)[a] | C5 | 7159 (39) | −468 (24) | 4651 (27) | 90 (25) |
| Ag2 | 4960 (3) | 1802 (2) | 4283 (2) | 70 (3)[a] | C6 | 4498 (33) | −469 (19) | 3180 (23) | 48 (19) |
| Ag3 | 6758 (3) | 1757 (2) | 5012 (2) | 81 (3)[a] | C10 | 2263 (45) | 2252 (25) | 2575 (31) | 116 (29) |
| Ag4 | 6959 (3) | 800 (2) | 4374 (2) | 82 (3)[a] | C11 | 3400 (37) | 2550 (21) | 3743 (26) | 73 (23) |
| Ag5 | 4176 (3) | 766 (2) | 2744 (2) | 66 (3)[a] | C12 | 3533 (45) | 2972 (26) | 2550 (32) | 120 (29) |
| Ag6 | 8413 (4) | 2120 (2) | 4883 (3) | 99 (3)[a] | C20 | 8737 (41) | 400 (24) | 3659 (29) | 106 (28) |
| Ag7 | 3847 (3) | 79 (2) | 4297 (2) | 73 (3)[a] | C21 | 8117 (65) | 570 (38) | 2338 (47) | 93 (45) |
| Ag8 | 5627 (3) | 169 (2) | 4260 (2) | 91 (3)[a] | C22 | 9299 (69) | 1225 (40) | 3092 (48) | 137 (47) |
| S1 | 4233 (9) | 1548 (5) | 3306 (6) | 45 (8)[a] | C30 | 3763 (63) | 2254 (36) | 5316 (44) | 224 (47) |
| S2 | 6714 (9) | 813 (6) | 3274 (6) | 52 (8)[a] | C31 | 4848 (52) | 2699 (29) | 5933 (37) | 156 (35) |
| S3 | 5658 (10) | 2249 (6) | 5094 (7) | 65 (9)[a] | C32 | 4604 (72) | 2468 (41) | 6738 (50) | 267 (60) |
| S4 | 7960 (11) | 1355 (6) | 4955 (7) | 74 (9)[a] | C40 | 10031 (47) | 1551 (26) | 5877 (34) | 136 (32) |
| S5 | 6910 (9) | 81 (6) | 4987 (7) | 58 (8)[a] | C41 | 9618 (38) | 696 (23) | 6706 (27) | 90 (25) |
| S6 | 4445 (11) | 123 (7) | 3453 (7) | 71 (9)[a] | C42 | 9613 (41) | 565 (22) | 5324 (29) | 95 (25) |
| Si1 | 3333 (12) | 2481 (7) | 2934 (8) | 65 (7) | C50 | 8071 (51) | −1292 (31) | 4764 (37) | 168 (37) |
| Si2 | 8408 (15) | 874 (9) | 3056 (11) | 116 (9) | C51 | 8664 (51) | −563 (29) | 5765 (37) | 162 (37) |
| Si3 | 4516 (18) | 2264 (11) | 5965 (13) | 157 (12) | C52 | 7137 (46) | −1140 (26) | 5678 (32) | 129 (32) |
| Si4 | 9425 (13) | 1000 (8) | 5915 (9) | 88 (8) | C60 | 2670 (50) | −708 (30) | 3156 (35) | 160 (36) |
| Si5 | 7820 (14) | −863 (8) | 5245 (10) | 102 (8) | C61 | 3258 (39) | −480 (22) | 1978 (27) | 87 (24) |
| Si6 | 3509 (13) | −731 (8) | 2750 (9) | 88 (8) | C62 | 3731 (42) | −1338 (25) | 2709 (29) | 107 (27) |
| C1 | 4146 (32) | 2042 (19) | 2850 (22) | 46 (19) | O1 | 6674 (27) | 2100 (15) | 3753 (18) | 104 (16) |
| C2 | 7511 (33) | 1215 (19) | 3148 (23) | 54 (20) | Me1 | 6059 (31) | 2474 (17) | 3753 (20) | 132 (19) |
| C3 | 5518 (33) | 2104 (19) | 5859 (23) | 59 (21) | Me2 | 5805 (29) | 964 (17) | 5406 (20) | 130 (18) |
| C4 | 8305 (31) | 1158 (17) | 5752 (21) | 37 (18) | O2 | 5188 (32) | 966 (18) | 4730 (24) | 150 (20) |

[a] Equivalent isotropic $U$ defined as one-third of the trace of the orthogonalized $U_{ij}$ tensor.

**Table VI.** Selected Bond Lengths (Å) and Angles (deg) for $[AgSC(SiMe_2Ph)_3]_3$ (**5a**), $[AgSC(SiMe_3)_3]_4$ (**4a**), and $[AgSCH(SiMe_3)_2]_8$ (**3a**)

| $[AgSC(SiMe_2Ph)_3]_3 \cdot 0.5C_6H_6$ | | $[AgSC(SiMe_3)_3]_4$ | | $[AgSCH(SiMe_3)_2]_8$ | |
|---|---|---|---|---|---|
| Ag1···Ag2 | 3.015 (1) | Ag1···Ag2 | 3.331 (3) | Ag1···Ag2 | 3.094 (2) |
| Ag1···Ag3 | 3.035 (1) | Ag1···Ag4 | 3.301 (3) | Ag1···Ag4 | 2.917 (2) |
| Ag2···Ag3 | 3.237 (1) | Ag2···Ag3 | 3.296 (3) | Ag2···Ag3 | 2.904 (2) |
| | | Ag3···Ag4 | 3.322 (3) | Ag3···Ag4 | 3.062 (2) |
| A1–S1 | 2.529 (2) | Ag1–S1 | 2.362 (8) | Ag1–S1 | 2.401 (4) |
| Ag1–S3 | 2.492 (2) | Ag1–S4 | 2.372 (7) | Ag1–S4 | 2.418 (4) |
| Ag2–S1 | 2.529 (2) | Ag1–S1 | 2.396 (8) | Ag2–S1 | 2.393 (4) |
| Ag2–S3 | 2.492 (2) | Ag1–S2 | 2.394 (9) | Ag2–S2 | 2.410 (4) |
| Ag3–S1 | 2.418 (2) | Ag2–S1 | 2.382 (8) | Ag3–S1 | 2.403 (4) |
| Ag3–S2 | 2.427 (2) | Ag2–S2 | 2.360 (8) | Ag3–S2 | 2.393 (4) |
| | | Ag4–S3 | 2.374 (7) | Ag4–S3 | 2.387 (4) |
| | | Ag4–S4 | 2.383 (7) | Ag4–S4 | 2.406 (4) |
| S1–C1 | 1.91 (1) | S1–C1 | 1.84 (2) | S1–C10 | 1.86 (1) |
| Si1–C1 | 1.90 (1) | Si1–C1 | 1.91 (3) | Si1–C10 | 1.83 (1) |
| Si2–C1 | 1.948 (9) | Si2–C1 | 1.93 (3) | Si2–C10 | 1.87 (2) |
| Si3–C1 | 1.988 (9) | Si3–C1 | 1.94 (3) | | |
| S2–C2 | 1.884 (9) | S2–C1 | 1.854 (9) | S2–C20 | 1.86 (1) |
| Si4–C2 | 1.97 (1) | Si4–C2 | 1.80 (2) | Si3–C20 | 1.85 (2) |
| Si5–C2 | 2.00 (1) | Si5–C2 | 1.99 (2) | Si4–C20 | 1.89 (2) |
| Si6–C2 | 1.89 (1) | Si6–C2 | 1.97 (2) | | |
| S3–C3 | 1.91 (1) | S3–C3 | 1.905 (8) | S3–C30 | 1.87 (1) |
| Si7–C3 | 1.954 (9) | Si7–C3 | 1.89 (1) | Si5–C30 | 1.86 (2) |
| Si8–C3 | 1.947 (8) | Si8–C3 | 1.89 (1) | Si6–C30 | 1.86 (2) |
| Si9–C3 | 1.92 (1) | Si9–C3 | 1.93 (1) | | |
| | | S4–C4 | 1.886 (7) | S4–C40 | 1.85 (1) |
| | | Si10–C4 | 1.922 (8) | Si7–C40 | 1.88 (2) |
| | | Si11–C4 | 1.870 (9) | Si8–C40 | 1.87 (2) |
| | | Si12–C4 | 1.921 (9) | | |
| Ag2–Ag1–Ag3 | 64.7 (1) | Ag2–Ag1–Ag4 | 89.5 (1) | Ag2–Ag1–Ag4 | 90.8 (1) |
| Ag1–Ag2–Ag3 | 57.9 (1) | Ag1–Ag2–Ag3 | 90.3 (1) | Ag1–Ag2–Ag3 | 88.5 (1) |
| Ag2–Ag3–Ag1 | 57.4 (1) | Ag2–Ag3–Ag4 | 89.8 (1) | Ag2–Ag3–Ag4 | 91.7 (1) |
| | | Ag3–Ag4–Ag1 | 90.3 (1) | Ag3–Ag4–Ag1 | 88.9 (1) |
| | | S1–Ag1–S4 | 176.8 (3) | S1–Ag1–S4 | 176.2 (1) |
| S1–Ag1–S3 | 163.1 (1) | S1–Ag2–S2 | 178.1 (3) | S1–Ag2–S2 | 175.6 (1) |
| S1–Ag2–S2 | 149.9 (1) | S2–Ag3–S3 | 176.5 (3) | S2–Ag3–S3 | 175.9 (1) |
| S2–Ag3–S3 | 153.6 (1) | S3–Ag4–S4 | 178.5 (3) | S3–Ag4–S4 | 174.7 (1) |
| | | Ag1–S1–Ag2 | 88.9 (3) | Ag1–S1–Ag2 | 80.4 (1) |
| Ag1–S1–Ag2 | 75.1 (1) | Ag2–S2–Ag3 | 87.3 (3) | Ag2–S2–Ag3 | 74.2 (1) |
| Ag2–S2–Ag3 | 83.6 (1) | Ag3–S3–Ag4 | 89.1 (3) | Ag3–S3–Ag4 | 79.7 (1) |
| Ag1–S3–Ag3 | 76.3 (1) | Ag4–S4–Ag1 | 87.9 (2) | Ag4–S4–Ag1 | 74.4 (1) |

and the cross-linking segments. It appears that, with the exception of the most severely constrained system **5a**, the octanuclear cyclic structure $[AgSR]_4$ constitutes the fundamental building block of these silver–thiolate structures. As steric constraints are relaxed, a gradual progression from the molecular structure of **4a**, to the associated biscyclic structure of **3a**, to the complex polymeric **2b** is observed as a consequence of the increased efficiency of secondary Ag···S bonding.

The charge requirements of **2b** are satisfied by the presence of methoxy groups in the crystal lattice. One methoxy unit displays

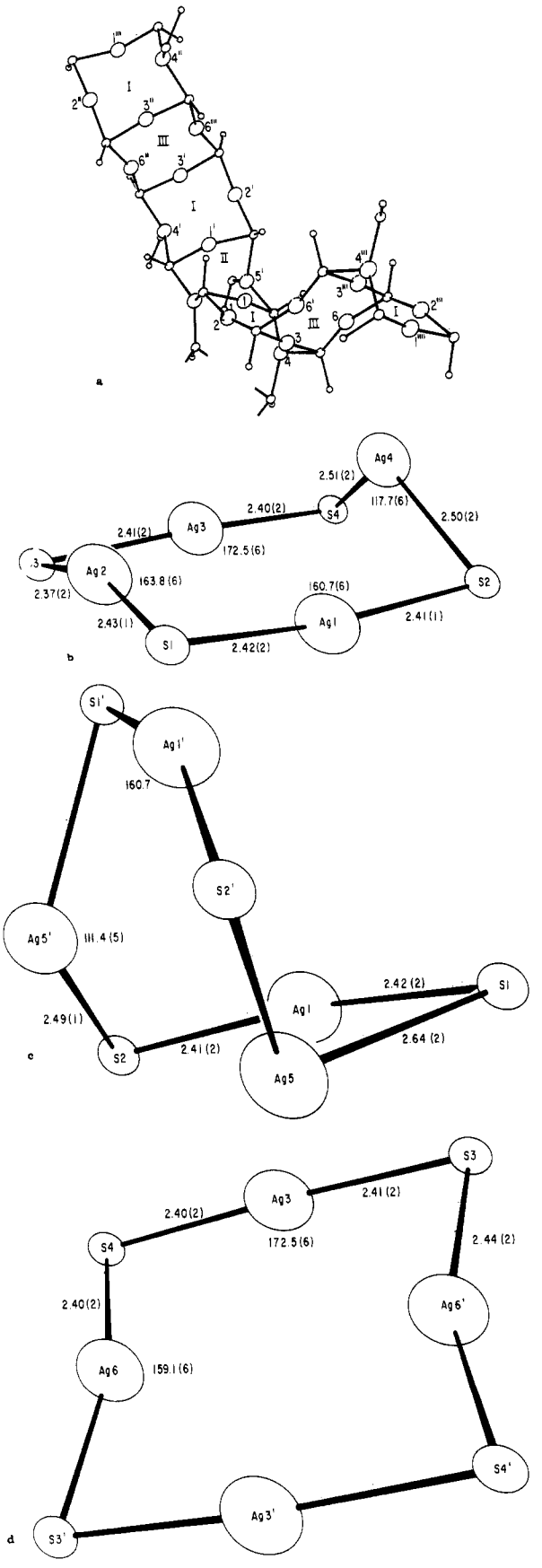


**Figure 7.** (a) Protion of the kinked chain of fused $Ag_4S_4$ cycles. (b) Schematic representation of the Ag1S1Ag2S2Ag3S3Ag4S4 cycle (I) with relevant molecular dimension. (c) Schematic representation of the Ag1S1Ag5S2′Ag1′S1′Ag5′S2 cycle (II) with relevant bond lengths and angles. (d) A view of the Ag3S3Ag6′S4Ag3′S3′Ag6S4 cycle (III) with relevant molecular dimensions.

**Table VII**

(a) Secondary Ag···S Interactions (Å) for $[AgSCH(SiMe_3)_2]_8$ (**3a**)

| | | | |
|---|---|---|---|
| Ag1···S2′ | 3.232 (1) | Ag···S4′ | 3.383 (1) |
| Ag2···S2′ | 3.298 (1) | Ag4···S4′ | 3.166 (1) |

(b) Intercycle Ag···Ag Distances (Å) for $[AgSCH(SiMe_3)_2]_8$ (**3a**)

| | | | |
|---|---|---|---|
| Ag1···Ag3′ | 3.570 (1) | Ag4···Ag4′ | 3.692 (1) |
| Ag2···Ag2′ | 3.506 (1) | | |

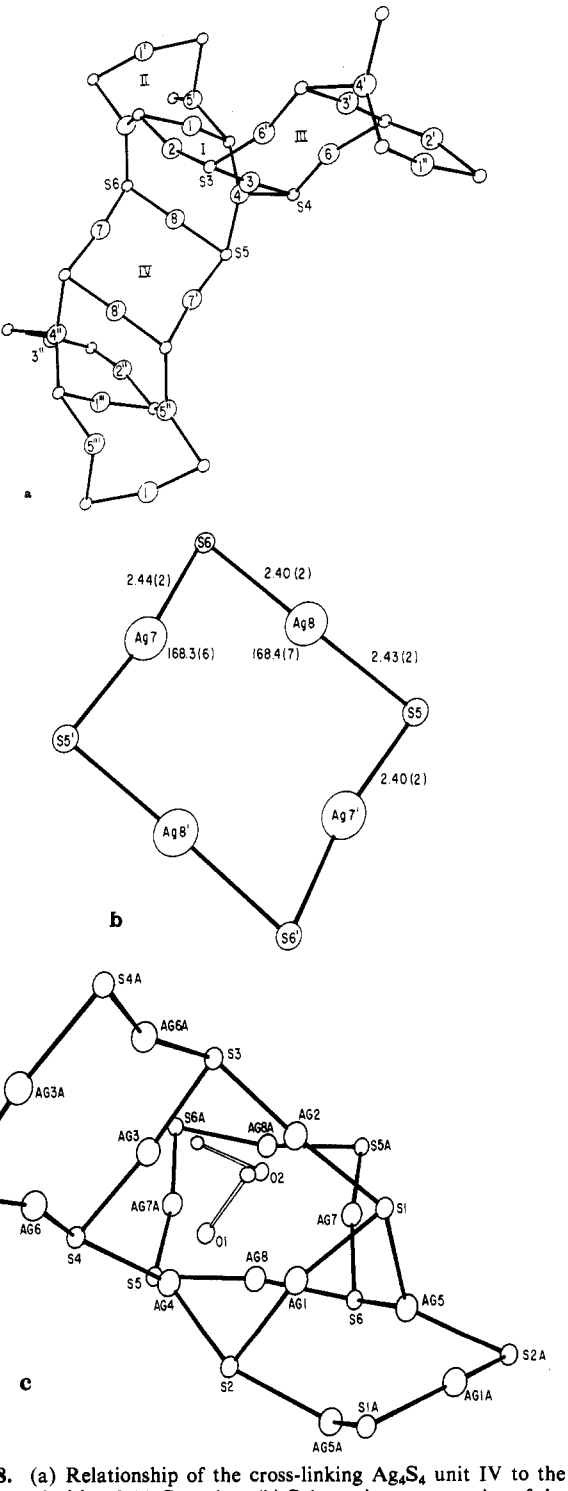


**Figure 8.** (a) Relationship of the cross-linking $Ag_4S_4$ unit IV to the kinked strand of fused $Ag_4S_4$ cycles. (b) Schematic representation of the Ag7S6Ag8S5Ag7′S6′Ag8′S5′ monocycle (IV) giving relevant bond lengths and angles. (c) Orientation of the methoxy units relative to the $Ag_4S_4$ cycles.

long Ag–O contacts in the range 2.99–3.08 Å, while the second exhibits weak interactions with Ag2 and Ag8, with Ag–O distances of 2.67 (5) and 2.77 (5) Å, respectively. To our knowledge, this is the first example of a cationic silver–thiolate complex, with the

**Table VIII.** Comparison of Relevant Structural Parameters for Neutral Homoleptic Silver(I)–Thiolate Complexes $[AgSR]_n$

| compd | Ag···Ag, deg | Ag–S, Å | S–Ag–S, deg | Ag–S–Ag, deg | S–C, Å | ref |
|---|---|---|---|---|---|---|
| $[AgSC_6H_{13}]_\infty$ | 3.232 (8) | 2.37 (1) | 173.2 (34) | 102.8 (20)[a]<br>87.2 (17) | 1.90 (10) | 5 |
| $[AgSC_6H_{11}]_{12}$ | 3.061 (15) | 2.40 (2)[b]<br>2.57 (2)[c] | 168[b] | 96 | | 1 |
| $[AgSCH(SiMe_3)_2]_8$ | 3.078 (1)[d]<br>2.911 (1)[d]<br>3.589 (1)[e] | 2.401 (7) | 175.6 (4) | 77.2 (7) | 1.86 (1) | *j* |
| $[AgSC(SiMe_3)_3]_4$ | 3.313 (6) | 2.378 (16) | 177.5 (12) | 88.3 (15) | 1.871 (1) | *j* |
| $[AgSC(SiPhMe_2)_3]_3$ | 3.025 (2)[f]<br>3.237 (1)[g] | 2.511 (4)[f]<br>2.42 (3)[g] | 163.1 (1)[f]<br>151.8 (2)[g] | 75.7 (2)[h]<br>83.6 (1)[i] | 1.90 (2) | *j* |

[a] The Ag–S–Ag angles are of two types: those at the sulfur atoms in the planar segment of the strand and those at the sulfur atoms in the crossover segments, 102.8 and 87.2°, respectively. [b] Entries refer to parameters for two-coordinate Ag atoms. [c] Entry refers to the three-coordinate silver center. [d] Entries refer to the two distinct Ag···Ag distances within each tetranuclear cycle. [e] Entries refer to Ag···Ag distances between cycles. [f] Entries refer to parameters for Ag1. [g] Entries for Ag2 and Ag3. [h] Average for S1 and S3. [i] Valence angle at S2. [j] This work.

**Table IX.** Selected Bond Lengths (Å) and Angles (deg) for $[Ag_4\{SCH_2(SiMe_3)\}_3]_n(OCH_3)_n$ (**2b**)

| | | | |
|---|---|---|---|
| Ag1···Ag2 | 3.055 (8) | Ag6–S4′ | 2.40 (2) |
| Ag1···Ag4 | 3.232 (7) | Ag6–S3′ | 2.44 (2) |
| Ag1···Ag5 | 2.940 (7) | Ag7–S6 | 2.44 (2) |
| Ag1···Ag5′ | 3.100 (7) | Ag7–S5′ | 2.40 (1) |
| Ag2···Ag3 | 3.119 (7) | Ag8–S5 | 2.43 (2) |
| Ag3···Ag4 | 3.249 (8) | Ag8–S6 | 2.40 (2) |
| Ag3···Ag6 | 3.096 (9) | Ag2···O2 | 2.67 (8) |
| Ag3···Ag6′ | 3.336 (9) | Ag8···O2 | 2.77 (5) |
| Ag4···Ag8 | 2.892 (8) | Ag1···O1 | 3.00 (4) |
| Ag5···Ag5′ | 3.279 (11) | Ag3···O1 | 3.08 (4) |
| Ag7···Ag8 | 3.064 (8) | Ag6′···O1 | 2.99 (5) |
| Ag7···Ag8′ | 3.350 (7) | S1–C1 | 1.79 (6) |
| Ag1–S1 | 2.42 (2) | S2–C2 | 1.87 (6) |
| Ag1–S2 | 2.41 (2) | S3–C3 | 1.90 (6) |
| Ag2–S1 | 2.43 (1) | S4–C4 | 1.90 (5) |
| Ag2–S3 | 2.37 (2) | S5–C5 | 1.89 (7) |
| Ag3–S3 | 2.41 (2) | S6–C6 | 1.87 (6) |
| Ag5–S4 | 2.40 (2) | C1–Si1 | 1.94 (6) |
| Ag4–S2 | 2.50 (2) | C2–Si2 | 1.88 (6) |
| Ag4–S4 | 2.51 (2) | C3–Si3 | 1.85 (6) |
| Ag4–S5 | 2.57 (2) | C4–Si4 | 1.91 (6) |
| Ag5–S1 | 2.64 (2) | C5–Si5 | 1.95 (7) |
| Ag5–S6 | 2.48 (2) | C6–Si6 | 1.90 (5) |
| Ag5–S2′ | 2.49 (1) | | |
| S1–Ag1–S2 | 160.6 (6) | S1–Ag5–S6 | 110.8 (5) |
| S1–Ag2–S3 | 163.8 (6) | S1–Ag5–S2′ | 111.5 (5) |
| S3–Ag3–S4 | 172.6 (6) | S2′–Ag5–S6 | 130.5 (6) |
| S2–Ag4–S4 | 117.7 (6) | S3′–Ag6–S4 | 159.0 (6) |
| S2–Ag4–S5 | 124.4 (6) | S5′–Ag7–S6 | 168.4 (6) |
| S4–Ag4–S5 | 110.3 (5) | S5–Ag8–S6 | 168.4 (7) |

stoichiometry $[Ag_4(SR)_3]^+(OMe)^-$.

The potential for a rich coordination chemistry of the new ligand types $(R_3Si)_2CHS^-$ and $(R_3Si)_3CS^-$ is now being realized in the isolation of metal–thiolate species inaccessible with conventional thiolates. The unusual group IV (group 14[24]) metal thiolate $[Pb(NR_2)(\mu\text{-}SCR_3)]_2$[9b] and the lithium thiolates of the type $[(R_3Si)_3CS)_4Li_2(THF)_n]$[9a] provide additional examples of the ability of this ligand type to stabilize unusual metal geometries.

Although there is a suggestion that the steric bulk of the substituent may be tailored to create particular degrees of aggregation, this view may be overly simplistic. Thus, mercury(II) 2-methyl-2-propanethiolate is polymeric[20] while mercury(II) ethanethiolate exhibits an essentially molecular structure.[21] Likewise, reaction conditions have been demonstrated to have a profound influence on the nature of metal–thiolate complexes.[22] Steric effects may predominate in certain cases, but other factors (charge, stoichiometry, solvent) may also play crucial roles in determining the degree of association of metal–thiolate species.

**Acknowledgment.** We thank the NSF for funding the 300-MHz NMR spectrometer. E.B. gratefully acknowledges support from the NSF, the donors of the Petroleum Research Fund, administered by the American Chemical Society, the Société Nationale Elf Aquitaine, and the John Simon Guggenheim Memorial Foundation. J.Z. and E.B. gratefully acknowledge partial support from the NIH (Grant GM2256608).

**Supplementary Material Available:** Tables listing bond lengths and angles and anisotropic temperature factors for structures **5a**, **4a**, **3a**, and **2b** and tables of derived hydrogen positions for **4a** and **3a** (31 pages); tables of calculated and observed structure factors for the structures (208 pages). Ordering information is given on any current masthead page.

(24) The periodic group notation in parentheses is in accord with recent actions by IUPAC and ACS nomenclature committees. A and B notation is eliminated because of wide confusion. Groups IA and IIA become groups 1 and 2. The d-transition elements comprise groups 3 through 12, and the p-block elements comprise groups 13 through 18. (Note that the former Roman number designation is preserved in the last digit of the new numbering: e.g., III → 3 and 13.)